Published online 3 January 2007 *Nucleic Acids Research, 2007, Vol. 35, No. 3* ***801–811***
doi:10.1093/nar/gkl1014

DNA methylation immediately adjacent to active histone marking does not silence transcription

Arie B. Brinkman, Sebastiaan W. C. Pennings, Georgia G. Braliou, Luc E. G. Rietveld and Hendrik G. Stunnenberg*

Department of Molecular Biology, Nijmegen Centre for Molecular Life Sciences, Radboud University, The Netherlands

Received August 2, 2006; Revised October 27, 2006; Accepted November 1, 2006

ABSTRACT

Active promoters generally contain histone H3/H4 hyperacetylation and tri-methylation at H3 lysine 4, whereas repressed promoters are associated with DNA methylation. Here we show that the repressed erythroid-specific carbonic anhydrase II (CAII) promoter has active histone modifications localized around the transcription start, while high levels of CpG methylation are present directly upstream from these active marks. Despite the presence of active histone modifications, the repressed promoter requires hormone-induced activation for efficient preinitiation complex assembly. Transient and positional changes in histone H3/H4 acetylation and local changes in nucleosome density are evident during activation, but the bipartite epigenetic code is stably maintained. Our results suggest that active histone modifications may prevent spreading of CpG methylation towards the promoter and show that repressive DNA methylation immediately adjacent to a promoter does not necessarily repress transcription.

INTRODUCTION

Chromatin is the physiologically relevant substrate for all genetic processes in eukaryotic cells. It represents a signal transduction platform for extracellular or intracellular signals and regulates all genome functions. While DNMTs methylate DNA, histone-acetyltransferases, histone-deacetylases, histone-methyltransferases and histone-demethylases determine the acetylation and methylation state of histones, the key protein component of chromatin. The specific combinations of resulting (post-translational) modifications are thought to provide transient or heritable epigenetic patterns that specify genome function. Emerging evidence causally links epigenetic alterations of chromatin to a disturbed proliferation–differentiation balance implicated in many diseases, providing the rational for the development of epigenetic treatment strategies using DNA-demethylating agents and HDAC inhibitors (1,2).

Several studies have identified the presence of acetylated histones H3/H4 and tri-methylated histone H3 lysine 4 (H3K4me3) co-localizing at 5′ regions of active genes, suggesting that these marks together represent an active code (3–9). However, the identification of these marks also at inactive genes suggests that the presence of these marks does not necessarily correlate ongoing transcription *per se* (10,11), and may as well represent a poised state.

Methylation of promoter CpG islands has been conceptually linked to gene silencing (12–14). Importantly, methylation seems to function as the dominant event that seals transcriptional repression. Methyl DNA-binding (MBD) proteins such as MeCP2 and MBD2 are known to be part of co-repressor complexes that specifically associate with methylated CpGs, contain HDAC activity and establish a repressive chromatin configuration (13,15–18).

We have previously shown that the erythroid-specific carbonic anhydrase II (CAII) is silenced through the action of the NCoR–SMRT co-repressor complex containing HDAC3 at an intronic enhancer and through a MeCP2–Sin3B co-repressor complex containing HDAC2 at the CAII promoter (19). Despite the presence of multiple HDAC-containing co-repressor complexes, the silenced CAII promoter was shown to be hyperacetylated. Here we have studied the epigenetic code in detail and show that it consists of H3/H4 acetylation as well as high levels of H3K4me3 around and downstream of the transcription start site. However, efficient preinitiation complex assembly takes place only after ligand-induced transcriptional activation of the promoter, and is accompanied by transient and positional changes in acetylation and local nucleosome density. Interestingly, while the upstream part of the CpG island is highly DNA-methylated, the region of the CpG island carrying active histone marks is maintained DNA methylation-free. This bipartite epigenetic

*To whom correspondence should be addressed at Nijmegen Centre for Molecular Life Sciences 191, PO Box 9191, Nijmegen 6500HB, The Netherlands. Tel: +31 24 3610524; Fax: +31 24 3610520; Email: h.stunnenberg@ncmls.ru.nl
Present addresses:
Georgia G. Braliou, Department of Biochemistry, Medical School, University of Thessaly Larissa, Greece
Luc E. G. Rietveld, The Netherlands Organization for Health Research and Development Den Haag, The Netherlands

code is largely unaffected by transcriptional activation of the promoter, implying that localized DNA methylation—even when adjacent to the transcription start site—is not necessarily a hallmark of gene silencing.

MATERIALS AND METHODS

Cell culture

HD3 and HD3-V3 cells were cultured in S13 medium consisting of Iscove's Modified Dulbecco's Medium (IMDM) supplemented with 10% fetal calf serum, 2% chicken serum, 0.7% BSA, 0.2% $NaHCO_3$, 120 μg/ml tranferrine (conalbumine), 110 μM β-mercaptoethanol. Before T3-treatment, HD3-V3 cells were cultured for 48 h in medium containing serum stripped by anion-ion exchange using AG 1-X8 resin (Bio-Rad). T3 was added to the medium to a final concentration of 500 nM where indicated. For AZAdC treatment cells were cultured for 5 days in the presence of 500 nM AZAdC. T2EC cells were cultured as described previously (20).

Chromatin immunoprecipitations

ChIP experiments were performed at least three times using independent chromatin preparations. Histone modification ChIPs and reChIPs were performed exactly as described previously (11). DNA recovered from ChIP was subjected to quantitative real-time PCR using iQ SYBR Supermix and a single-color detection MyIQ iCycler (Bio-Rad, Hercules, CA, USA). The following formula was calculated using $[\%\text{ChIP/input}] = [E^{(Ct_{input} - Ct_{ChIP})} * 100\%]$, where E represents the primer efficiency, as determined for every primerset.

Mononucleosomal chromatin was prepared by the same cross-linking procedure. Cells were washed once with PBS, once with 5 ml NP-40 lysisbuffer (10 mM Tris, pH 7.4, 10 mM NaCl, 3 mM $MgCl_2$ and 0.5% NP-40), once with 2.5 ml of micrococcal nuclease (MNase) digestion buffer (10 mM Tris, pH 7.4, 15 mM NaCl and 60 mM KCl), and resuspended in 1 ml of the same buffer with 1 mM $CaCl_2$ at room temperature. MNase (200 units; Worthington) was added and chromatin was digested to mononucleosomal size for 30 min at room temperature. The digestion was stopped by the addition of 1 ml stop buffer (100 mM Tris, pH 8.0, 20 mM EDTA, 2% SDS and protease inhibitors). After centrifuging for 10 min at room temperature the resulting supernatant was used for reChIP experiments.

For transcription factor ChIPs the following protocol was used. Cells were collected and adjusted to 5×10^6 cells/ml in culture medium. Cross-linking was done by adding 0.1 volof buffer A (50 mM HEPES, pH 7.6, 100 mM NaCl, 1 mM EDTA, 0.5 mM EGTA and 11% formaldehyde) and incubated at room temperature for 30 min. Cross-linking was stopped by the addition of glycine to a final concentration of 125 mM and incubation for 5 min at room temperature. Cells were washed once with ice-cold PBS, once with buffer B (20 mM HEPES, pH 7.6, 0.25% Triton X-100, 10 mM EDTA and 0.5 mM EGTA), and once with buffer C (50 mM HEPES, pH 7.6, 150 mM NaCl, 1 mM EDTA and 0.5 mM EGTA). Washings consisted of a 10 min rotation and a 7 min spin at 500 *g* (1200 r.p.m.) at 4°C. The obtained nuclei were resuspended in buffer D (20 mM HEPES, pH 7.6, 1 mM EDTA, 0.5 mM EGTA, protease inhibitors and 0.05% SDS added freshly) to 20×10^6 nuclei/ml and sonicated 11 times for 10 s on ice-ethanol. The sonicated chromatin was centrifuged for 5 min at 14 000000 *g* at 4°C. The supernatant was used directly for ChIP or stored at −80°C. In a final volume of 300 μl, 100 μl of chromatin was mixed with, 60 μl of 5× incubation buffer (50 mM Tris–HCl, pH 8.0, 750 mM NaCl, 5 mM EDTA, 2.5 mM EGTA, 5% Triton X-100 and 0.75% SDS), 6 μl of 5% BSA, protease inhibitors and 30 μl of 33% Protein A/G–agarose slurry. Before use Protein A/G–agarose beads were washed twice with 1× incubation buffer, 0.1% BSA twice for at least 2 h at 4°C. After preclearing for 2 h at 4°C the supernatant was collected, the appropriate antibody and 30 μl of 33% Protein A/G–agarose slurry were added and samples were rotated overnight at 4°C. Protein A–agarose beads containing the immune complexes were washed twice with wash buffer 1 (10 mM Tris–HCl, pH 8.0, 150 mM NaCl, 1 mM EDTA, 0.5 mM EGTA, 1% Triton X-100, 0.1% SDS, 0.1% DOC and protease inhibitors), once with buffer 2 (as buffer 1, but with 500 mM NaCl), once with buffer 3 (10 mM Tris–HCl, pH 8.0, 1 mM EDTA, 0.5 mM EGTA, 0.5% DOC, 0.5% NP-40, 250 mM LiCl and protease inhibitors), and twice with buffer 4 (10 mM Tris–HCl, pH 8.0, 1 mM EDTA, 0.5 mM EGTA and protease inhibitors). Subsequent elution, DNA purification and PCR analysis were performed as for histone modification ChIPs described above.

Antibodies. The following antibodies were used: 2 μg of anti-H3K9ac or anti-H4ac (Upstate #06-942 or #06-866, respectively); 1 μg of anti-H3K4me1, anti-H3K4me2, anti-H3K4me3 and anti-histone H3 (Abcam ab8895, ab7766, ab8580 and ab1791, respectively); 2 μg of anti-H3K9me3 [#4861 (21) a gift from T. Jenuwein], 2 μg of anti-TBP, 10 μg of anti-TFIIA, 6 μg of anti-TFIIB, 6 μg of anti-RNAPII-CTDser5-P and 2 μg of anti-RNAPII-CTD.

Oligonucleotides

The following oligonucleotides were used for quantitative real-time PCR: NC3 (−7 kb), 5′-GCAGACACTGGCAGGTTTC-3′; NC4 (−7 kb), 5′-TATGAGCCTTAGCCTTAG-3′; CT1 (−4 kb), 5′-CATGTAGTCAAGGTTGTT-3′; CT2 (−4 kb), 5′-CTCATGGCATATCAGTGC-3′; CAII −1.0 kb A, 5′-ACTCACAGTGGCCAGCAGAGTT-3′; CAII −1.0kb B, 5′-CGGCGTTTTATCCCATCTTT-3′; 5A (−0.5 kb), 5′-CGGGAAAGCACACTCTCA-3′; 6B (−0.5 kb), 5′-GGAAGGGATTAGCGGGGA-3′; P16 (0 kb), 5′-CGGAGAAGGGCATGGAGTT-3′; P18 (0 kb), 5′-CCGGCTCCGTCGGCTATC-3′; CAII +0.5 kb A, 5′-ATCGCCATCAGCACCAAAG-3′; CAII +0.5 kb B, 5′-TGTCGGAGGAGTCGTCAAACT-3′; CAII +1.0 kb^2 F, 5′-TATGAGAACAGTTATAGGTATAG-3′; CAII +1.0 kb^2 R, 5′-TGTAATCCTCTGTTATTCTACAG-3′; CAII +6 kb F, 5′-CAGCTGAGCTAAGAGCCACTTG-3′; CAII +6 kb R, 5′-AGGTGTGAGTATGGCTGGGAA-3′; HS7 (+7 kb), 5′-TCTGGAACATCCTTGCTA-3′; 3P (+7 kb), 5′-AGCGGATGATGTAGAGAT-3′; CAII 8 kb^2 F, 5′-ATGTGACTGCTGCCACTTCCT-3′; CAII 8 kb^2 R, 5′-TCCCATGCAGAACAGGGC-3′; GL6.241a (β-globin), 5′-GGGTCCGACCAGGAAGGA-3′; GL6.241b (β-globin), 5′-TCAGTGCCAGGATTGAAGCA-3′; 36882-F (β-globin),

5′-TGACACTGGAAACCTATGGCC-3′; 36882-F (β-globin), 5′-AGCCCCGAGTGCAGGTGGA-3′; HinFI sat F, 5′-CCCCACACGGACAAATTCA-3′; HinFI sat R, 5′-GAAATACCTTACGCCCAGGAGA-3′. For bisulphite sequencing three PCR fragments encompassing the CAII promoter CpG island were generated using nested PCR with the following primers: CAII BSS5 F, 5′-TYGGTGATGTTATTTTAGATTTATAGTGG-3′; CAII BSS5 R, 5′-CCCCTAATTCTTACTTAAAAATATACTTTCC-3′; CAII BSS6 F, 5′-TAGAGTTYGGGTTAYGGGGTTG-3′; CAII BSS6 R, 5′-ATAAAACRATACTCACRTTCACTCACC-3′; CAII BSS8 F, 5′-TYGTGGGAGTGGTGATTTAATTG-3′; CAII BSS8 R, 5′-CACCRCATCACRCRAACTCCC-3′; CAII BSS7 F, 5′-YGYGYGTTTTTTATAAGGTGAGTG-3′; CAII BSS7 R, 5′-AAACRCTACRACCTTAAACTAAAACAAC-3′; CAII BSS1 F, 5′-GAGTYGTTTTTAYGGTTTTTAGTAGGG-3′; CAII BSS1 R, 5′-CRTACCCCCAATAATAAAACATAATAC-3′; CAII BSS3 F, 5′-TTYGTYGTYGTTGTTTTAGTTTAAGG-3′; CAII BSS3 R, 5′-CRTAACCTCRACRAACTATCAAAAAC-3′.

Bisulphite sequencing

Less than 1 μg of sonicated genomic DNA was diluted to 50 μl in MQ. A small quantity measuring 5.7 μl of 3 M NaOH was added and the samples were incubated at 37°C for 10 min. Thirty-three microliters of 16 mM hydroquinone (freshly prepared) and 530 μl of 4 M sodium bisulphite solution (prepared by dissolving 3.8 g of $Na_2S_2O_5$ in 7 ml of MQ and adjusting the pH to 5.0 with 750 μl of 3 M NaOH) was added and samples were incubated at 50°C for 16–20 h. Samples were subsequently purified using QIAquick PCR purification columns and eluted with 50 μl MQ at 50°C. After the addition of 5.7 μl of 3 M NaOH, samples were incubated at 37°C for 15–20 min and subsequently precipitated using 17 μl of 10 M NH_4Ac, 450 μl of 96% EtOH and 20 μg of glycogen. After washing with 70% EtOH DNA was dissolved in 50 μl of MQ and used for PCR. The obtained PCR fragments were cloned and for each fragment 10 clones were sequenced. Sequences were analyzed using the MethTools program (22).

RESULTS

Locus-wide analysis of histone modifications in HD3 cells

We previously showed that repression of the CAII promoter correlates with the presence of the NCoR–HDAC3 co-repressor complex at the HS2 intronic enhancer and the MeCP2–Sin3–HDAC2 co-repressor at the promoter (see Figure 1). Despite the presence of the HDAC-containing co-repressor complex, the promoter is hyperacetylated (19). To extend this observation and to study the epigenetic state of the CAII locus in more detail we performed chromatin immunoprecipitation (ChIP) analysis followed by real-time PCR. We selected two upstream regions at −7 kb and at −4 kb known to be irrelevant to the regulation of CAII expression, several regions throughout the CpG island promoter from −1 to +1 kb, and around the downstream intronic enhancer from +6 kb to +8 kb (see Figure 1).

First, histone H3 lysine 9 methylation (H3K9me3) was analyzed. Although this mark has been extensively correlated with repression, it has also been detected by others and us in coding regions of active genes (11,23). Although an inverse pattern compared with H3K4 tri-methylation seemed to be present (Figure 2B), the overall levels of H3K9me3 were only moderate. Whereas a positive control region for H3K9me3 (HinFI satellites) showed ∼30% recovery, positions within the CAII locus showed only 5–10% recovery. The β-globin 36 882 position has been described as condensed (H3K9-dimethylated) (24), but at this position we found H3K9me3 to be as low as within the CAII locus.

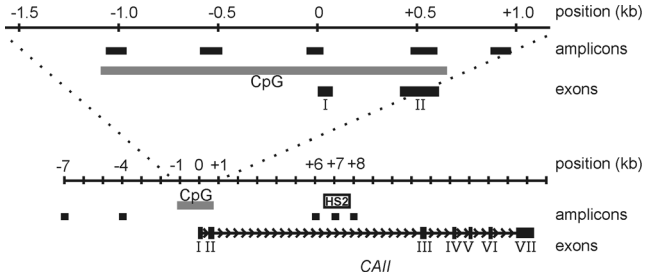

Figure 1. The carbonic anhydrase II (CAII) locus. Black bars, amplicons used in ChIP experiments; gray bar, CpG island; open box, HS2 DNase I hypersensitive site identified previously (26). HS2 is an intronic enhancer that contains the v-ErbA response element. Positions relative to the transcription start are indicated. The structure of the CAII gene is outlined at the bottom with exons displayed as filled boxes.

Next, we analyzed methylation of histone H3 at lysine 4 (H3K4, Figure 2B) that can be either mono-, di- or tri-methylated. High levels of H3K4-tri methylation were observed at 0 kb and +1 kb (note the difference in the scale used in Figure 2A–C). Lower levels were observed for H3K4 di-methylation at 0 kb. H3K4 mono-methylation was absent at the promoter. Except for H3K4 mono methylation, levels at the CAII promoter were considerably higher than at the β-globin hyperacetylated/H3K4-dimethylated 6.241 position.

In addition to methylation, we analyzed acetylation that correlates with active loci. As we have shown previously, histones H3 and H4 were hyperacetylated at the promoter (0 and +1 kb, Figure 2C) (19). Extending these analyses, we now show that hyperacetylation is largely confined to the promoter region, although the level at the promoter in its silent state is lower when compared to the β-globin 6.241 position. Site-specific anti-acetylation antibodies revealed that histone H3 was predominantly acetylated at K9 whereas with histone H4, lysines 5, 8, 12 and 16 were acetylated to the same extent (data not shown).

Altogether, these results corroborate and extend our previous analyses showing that the promoter contains localized active histone modifications despite the presence of HDAC-containing co-repressor complexes recruited to the promoter and enhancer (19).

Histone modification changes during hormone-induced activation of CAII expression

As the results described above showed that active histone marks are already established under non-induced conditions, we set out to assess whether the histone modification pattern changes upon thyroid hormone-induced activation of CAII expression. We have previously shown that the expression of

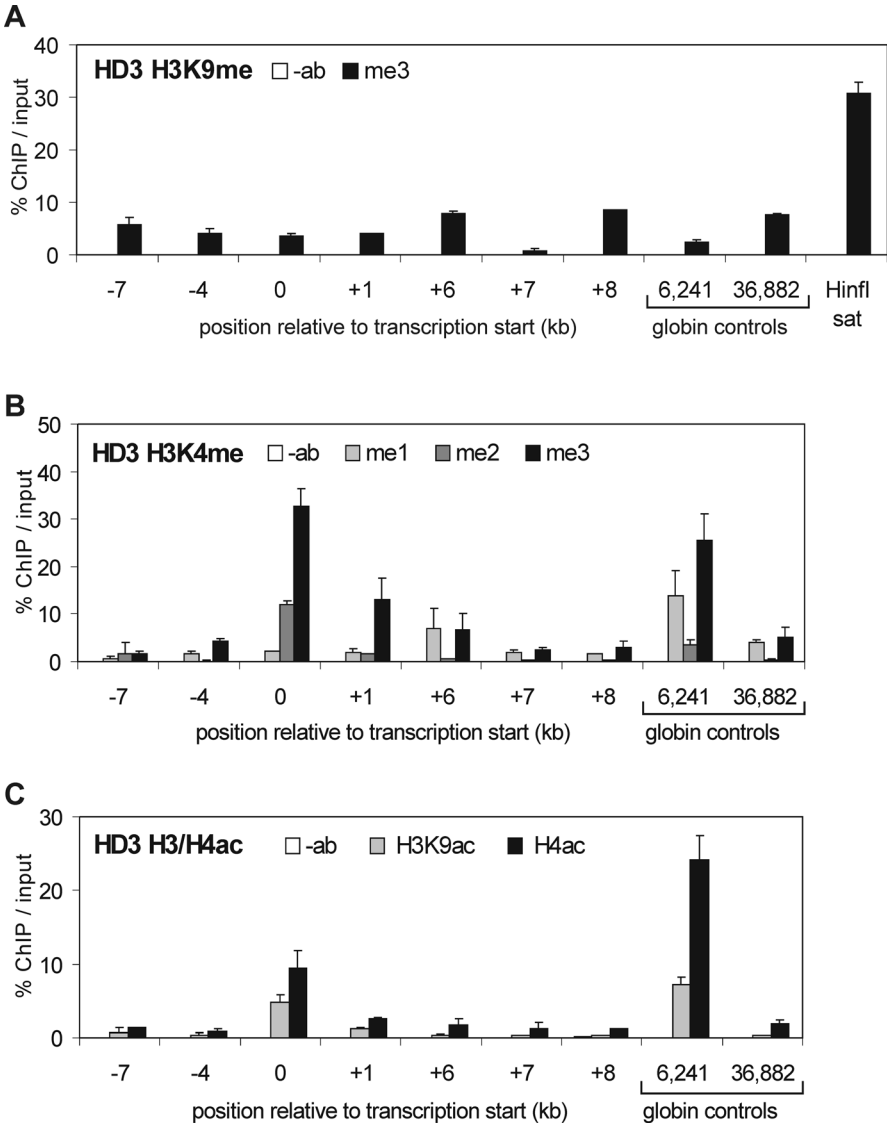

Figure 2. Analysis of histone modifications within the repressed CAII locus in HD3 cells. (**A**) Histone H3K9me3; −ab; no antibody control. (**B**) Histone H3K4me1, H3K4me2 and H3K4me3. (**C**) Histone H3K9ac and H4ac (K5, K8, K12, K16). Positions relative to the transcription start are indicated. 6241 is a hyperacetylated/H3K4-dimethylated site and 36 882 is a H3K9-dimethylated site in the chicken β-globin locus, respectively, as described by Litt *et al*. (24). HinFI sat, CR1-containing pericentromeric repeat element (32).

the CAII gene can be activated by T3 (thyroid hormone) in HD3-V3 cells, which are complemented with a hormone responsive gag-c-ErbA allele (25). This activation involved dissociation of the NCoR–HDAC3 co-repressor complex from the HS2 enhancer and replacement by a TRAP220-containing co-activator complex, whereas the MeCP2-targeted co-repressor complex remained bound to the CpG island at the promoter (19). To study the timing of this activation, we isolated total RNA from T3-induced HD3-V3 cells and analyzed CAII transcription using real-time RT–PCR and intronic primers to directly measure transcriptional activity. Induction was observed already after 5 min, with near-maximal induction after 30–60 min (Figure 3A).

Samples from this time-course experiment were used for histone code ChIP analysis. Since it was evident from Figure 2 that histone modifications associated with active chromatin are predominantly targeted to sequences surrounding the transcription start, we increased the resolution of our analysis within this region (−1 to +1 kb), which encompasses the complete CpG island, the transcription start site and part of the first intron (see Figure 1).

H3K9me3 levels within the upstream intergenic and promoter region remained constant over time (Figure 3B). However, downstream from the promoter H3K9me3 increased gradually upon induction. Clearly, H3K9me3 within the active CAII coding region is indicative of active rather then inactive chromatin. This observation confirms previous observations by others and us which showed H3K9me3 to be associated with transcription elongation (11,23). At the +7 HS2 enhancer position H3K9me3 did not increase. However, this position appears to be rather nucleosome-poor (see below and Figure 3F).

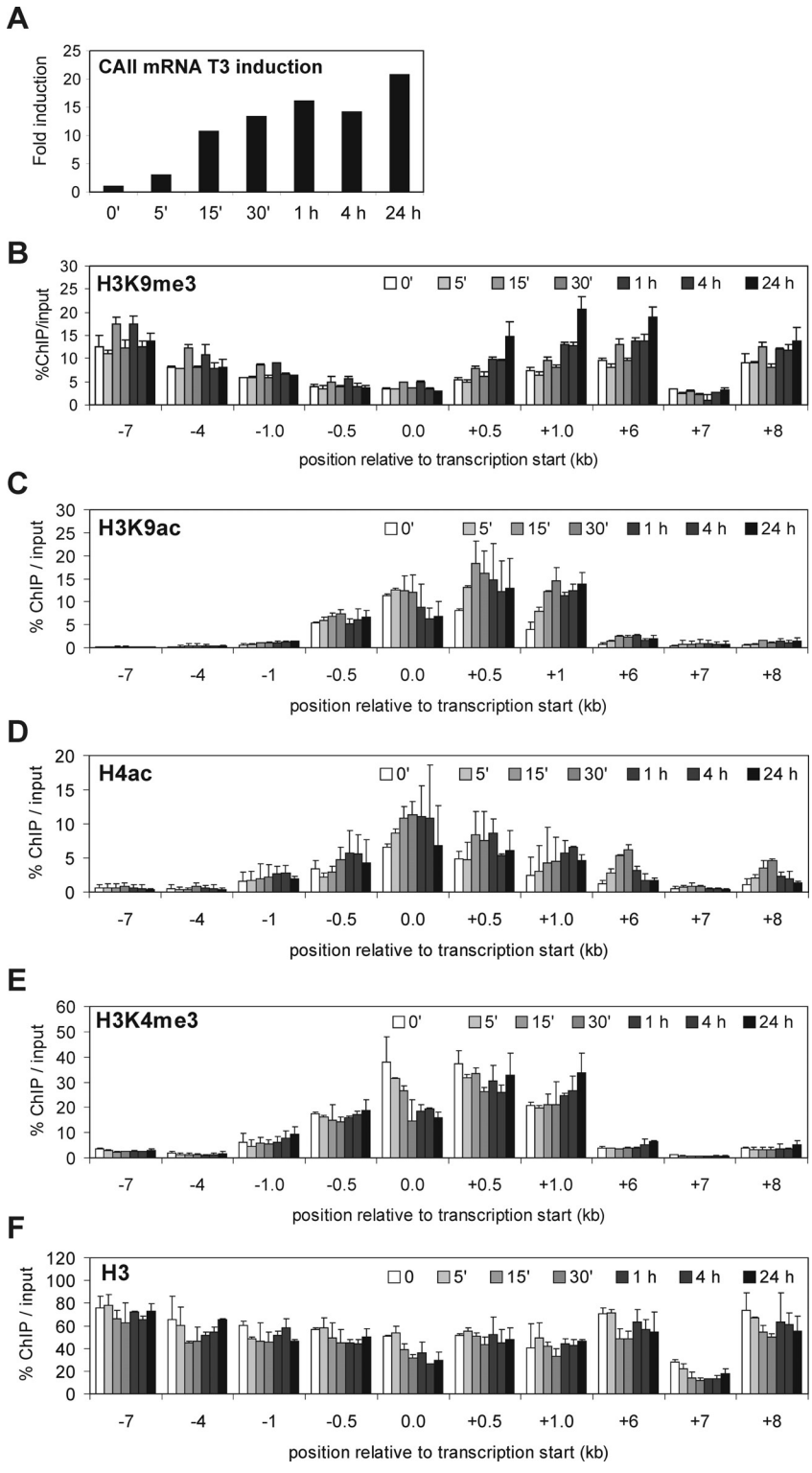

Figure 3. ChIP analysis of histone modifications upon hormone-induced activation of CAII transcription. (**A**) CAII transcription upon addition of T3 was quantified by real-time RT–PCR. An intronic primerset was used to monitor transcriptional activity. (**B**) Histone H3K9me3; (**C**) histone H3K9ac; (**D**) histone H4ac (K5, K8, K12, K16); (**E**) histone H3K4me3; and (**F**) histone H3 (C-terminus). Positions relative to the transcription start are indicated.

Changes in histone modification patterns associated with active chromatin remained restricted to the region surrounding the transcription start (Figure 3C–E) except for H4 acetylation that was also increased at gene internal positions upon gene expression (Figure 3D). Quantitative and positional changes were evident. H3K9 acetylation was highest at 0 kb in the absence of T3 (Figure 3C). At this position, a decrease of ~2-fold was apparent upon ligand induction. This decrease

was mirrored by a gradual increase of ~4-fold at the +1 kb position. Throughout induction, the highest levels of H4 acetylation remained at the transcriptional start site; positional changes as observed for H3K9 acetylation were not detected. H3K4 tri-methylation was found to be highest around the transcription start site and decreased upon ligand-induction (Figure 3E). Using a pan-H3 antiserum we monitored nucleosome density throughout the locus during T3-induction (Figure 3F). Constant levels of H3 were measured at most positions, although slightly higher values were present at −7, −4, +6 and +8 kb. At the transcriptional start the initial level was similar to surrounding positions but decreased gradually over time during induction, suggesting nucleosome disruption or eviction. This could explain why H3/H4ac and H3K4me3 locally decrease during induction, and it implicates that the initial increase in H4 acetylation is even more pronounced. At +7 kb H3 was initially low and slightly decreased further during induction. This position was previously identified as the HS2 DNase I hypersensitive site (26). Whereas high levels of the active histone modifications were present around and downstream from the transcription start site, the upstream regions including the distal region of the CpG island were almost devoid of these modifications. At −1 kb H3K4 tri-methylation and H3K9 acetylation were, respectively, 6-fold and 20-fold lower than measured at the transcriptional start site, and, respectively, 3-fold and 7-fold lower than at +1 kb. Since the resolution of our ChIP experiments is not >500 bp (the average DNA length of the chromatin used), it is possible that this transition is sharper than evident from Figure 3. The presence of this transition suggests that spreading of the active histone modifications in the upstream direction is actively prevented or alternatively that modifying enzymes are highly specifically targeted to the transcription start site. Finally, H3K4 mono- and di-methylation remained as low as in the repressed state (Figure 2 and data not shown), and a conversion from H3K4 di- to tri-methylation was not observed, as reported upon activation in yeast (3).

Taken together, H3K9 tri-methylation is unaffected within the upstream and promoter region upon activation, but is increased within the gene-coding region. H3/H4 acetylation and H3K4 tri-methylation co-localize over the transcriptional start site and immediate downstream region. Remarkably, the ligand-induced changes in the active code are not synchronous but appear to follow their own individual dynamics, while a modest but significant local nucleosome disruption or eviction is evident. The active histone modifications are absent at the distal part of the CpG island and beyond.

H3K9 acetylation, but not H3K9 tri-methylation, is simultaneously present on H3K4 tri-methylated nucleosomes

The results described above show that the active histone code—H3/H4 acetylation and H3K4 tri-methylation—may be confined to a few nucleosomes surrounding the transcriptional start site. In addition, moderate levels of H3K9 tri-methylation are present within the same region. To determine whether these marks are targeted to the same or distinct nucleosomes we performed consecutive ChIP experiments (reChIPs) on cross-linked mononucleosomal chromatin. After formaldehyde fixation of HD3 cells, mononucleosomal-sized chromatin was prepared using MNase digestion (see Figure 4A), subjected to a first-round ChIP, eluted and subjected to a second-round ChIP. As expected, a first-round ChIP using anti-H3K9ac or anti-H3K9me3 revealed that the −7.0 position contained H3K9me3 but low H3K9ac, while the 0.0 position contained H3K9me3 and high H3K9ac (Figure 4B, lanes 1–3). It should be noted that the H3K9ac ChIP with mononucleosomal chromatin was much more efficient than when using sonicated chromatin.

Next, anti-H3K9ac and anti-H3K9me3 were used in the first-round ChIP, followed by a second-round ChIP using anti-H3K4me3 (Figure 4B, lanes 4–6). H3K4me3 could be recovered only at the 0.0 position, and only after a first-round ChIP using anti-H3K9ac. At −7.0, H3K4me3 could not be recovered because this position was devoid of H3K9ac. These results provide strong evidence for the simultaneous presence of H3K9ac and H3K4me3 at the 0.0 position, and indicate that H3K9me3 and H3K4me3 (i.e. inactive and active marks) are unlikely to be present within the same nucleosomes. The detection of both H3K9me3 and H3K4me3 at the same positions in Figures 1 and 3, may be explained by the use of sonicated chromatin, which may contain more than one differentially modified nucleosomes.

Preinitiation complex assembly

The maintenance of active histone marks even under repressive conditions prompted us to determine whether the active histone marks signals the presence of basal transcription factors and/or a (partially) pre-assembled preinitiation complex. Therefore we analyzed the association of general transcription factors under repressed as well as activated conditions (Figure 5). General transcription factors were not associated with the inactive promoter, although a weak but reproducible level of TBP was observed under these conditions. The presence of a preinitiation complex (PIC) was evident after T3-treatment: TBP, TFIIB and TFIIA were detected at the transcription start, whereas RNAPII and

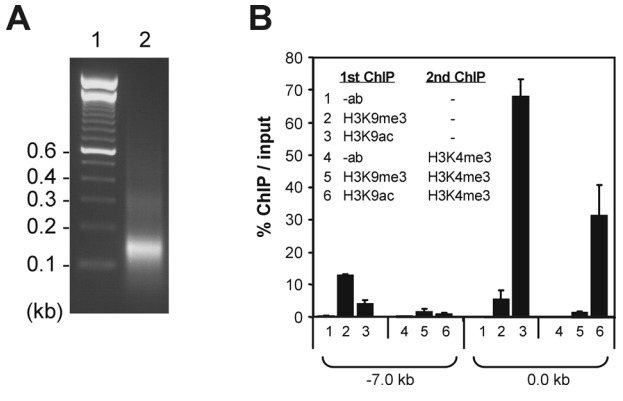

Figure 4. H3K9 acetylation and H3K4 tri-methylation are targeted to the same nucleosomes at the CAII promoter. (**A**) Mononucleosomal chromatin from HD3 cells. Lane 1, DNA marker; lane 2, micrococcal nuclease-digested chromatin. (**B**) ReChIP experiments. Mononucleosomal HD3 chromatin was subjected to a first-round ChIP, eluted and subjected to a second-round ChIP. The antibodies used for first- and second-round ChIPs are indicated. Recovered DNA was quantified using real-time PCR.

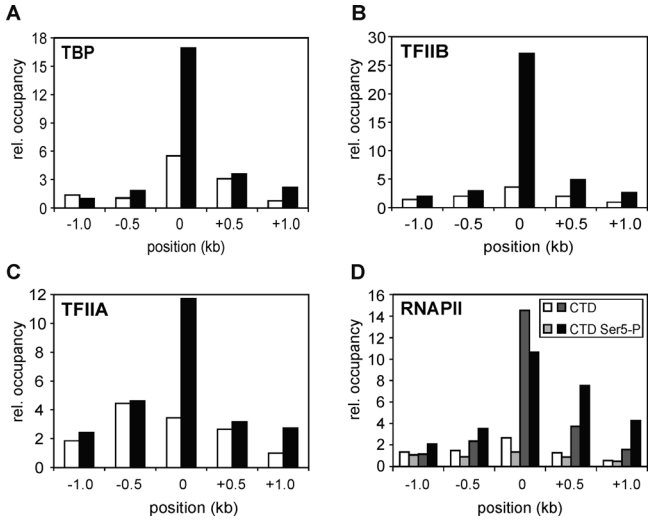

Figure 5. Assembly of the preinitiation complex at the CAII promoter. ChIP analysis was performed on HD3 cells (white and light gray bars) and 24 h T3-treated HD3-V3 cells (black and dark gray bars), in which CAII is repressed or induced, respectively. Values are expressed as occupancy relative to the −7 kb position. Positions relative to the transcription start site are indicated.

CTD-Ser5-phosphorylated RNAPII could in addition be detected at positions downstream from the transcription start, indicative of ongoing transcription. Thus, despite the active histone marks at the CAII promoter, full establishment of the PIC occurs only upon T3-treatment.

DNA methylation is restricted to the distal part of the CpG island

Our previous work indicated that the CpG island CAII promoter in its repressed state is partially DNA methylated and associated with a MeCP2–Sin3–HDAC2 co-repressor complex (19). These data seemingly contradict our present findings, since DNA hypermethylation of promoter-CpG islands is conceptually related to silencing of genes and heterochromatin formation, e.g. deacetylation of H3/H4 and methylation of H3K9. This apparent contradiction prompted us to reinvestigate in more detail the DNA methylation pattern at the CpG island containing the CAII promoter.

The CpG island is located from −1100 to +700 bp relative to the transcription start site (Figure 1). Although the upstream part of this CpG island (−1100 to −600) has a lower GC-content and observed/expected CpG ratio (56% and 0.8, respectively) than the downstream part (−600 to +700, 74% and 1.1, respectively), the upstream part still meets the criteria of a CpG island [≥200 bp in length, ≥50% GC and observed/expected CpGs ≥0.6 (27)]. Chicken CpG islands have higher GC-contents than those of mouse and human, but the upstream part or the CAII CpG island has 58% GC, which is well above the average of chromosome 2 [∼40% (28)]. Bisulphite sequencing showed that CpG hypermethylation was present within this upstream region of the CpG island (66% at −1091 to −600, Figure 6A). Remarkably, methylation was absent at the promoter-proximal region of the CpG island (−600 to −12), where CpG density is highest. Thus, the epigenetic state of the CpG island is bipartite: the upstream part is extensively CpG methylated and lacks active histone modifications, whereas the downstream promoter-proximal part is devoid of DNA methylation and contains active histone modifications. We previously reported that the CAII CpG island is associated with the MeCP2–Sin3–HDAC2 complex (19). This association most likely takes place at the upstream, methylated part. Notably, for ChIP analysis of MeCP2 a primerset located around position −500 was used in those experiments.

Next, we tested whether activation of transcription by T3 ligand caused loss of CpG methylation. Following induction, methylation in upstream part of the CpG island was largely maintained at 24 h after induction (55% CpG methylation, Figure 6B and C). We previously demonstrated that the DNA methylation inhibitor AZAdC causes (partial) dislodgement of MeCP2–Sin3 co-repressor complex and activation of CAII expression [Figure 7A and (19)]. We therefore tested whether an AZAdC-induced loss of CpG methylation would cause a concomitant increase in histone acetylation in the upstream part of the CpG island promoter. AZAdC treatment over a period of 5 days resulted in more than 6-fold increase of CAII gene expression (Figure 7A), and extensive loss of CpG methylation (from 66 to 18%), although some cells within the analyzed population appeared to have partially retained CpG methylation (Figure 6D). The same samples were used to analyze active histone modifications. The AZAdC treatment did not alter the position of these modifications, although quantitative changes of individual modifications were evident (Figure 7B). Whereas H4ac decreased locally at the transcription start site, H3Ac and H3K4me3 increased at all of the measured positions, with a maximum of 2-fold. Thus, CpG demethylation does not cause positional changes in the active histone marks, but rather appears to consolidate levels of these modifications.

Active histone marks but not the DNA methylation pattern is established in erythrocytic progenitor cells

The results described above showed that the bipartite epigenetic code is present in cells in which CAII expression is not induced, and persists during activation of gene expression. Moreover, active histone marks are stably maintained even when CpG methylation in the upstream part of the CpG island is removed. To test whether the bipartite organization of the described epigenetic pattern is already established earlier during differentiation, we analyzed active histone modifications and the DNA methylation pattern in chicken T2EC cells. These cells are very immature haematopoietic progenitor cells committed to the erythrocytic lineage and should be considered non-transformed (20).

The level of CAII expression in T2EC is about 9-fold higher than in HD3 cells (repressed state) but 4-fold lower than in T3-induced V3 cells (Figure 7A). Analysis of histone modifications in T2EC cells showed that the H3K9me3 pattern is essentially the same as in HD3 cells (Figure 8A). Only the gene-coding region has elevated H3K9me3, which is in agreement with the higher level of transcriptional elongation in T2EC cells (see Figure 7A). Active histone marks are also present in these cells, although peak levels were concentrated to a more upstream position; at −0.5 kb

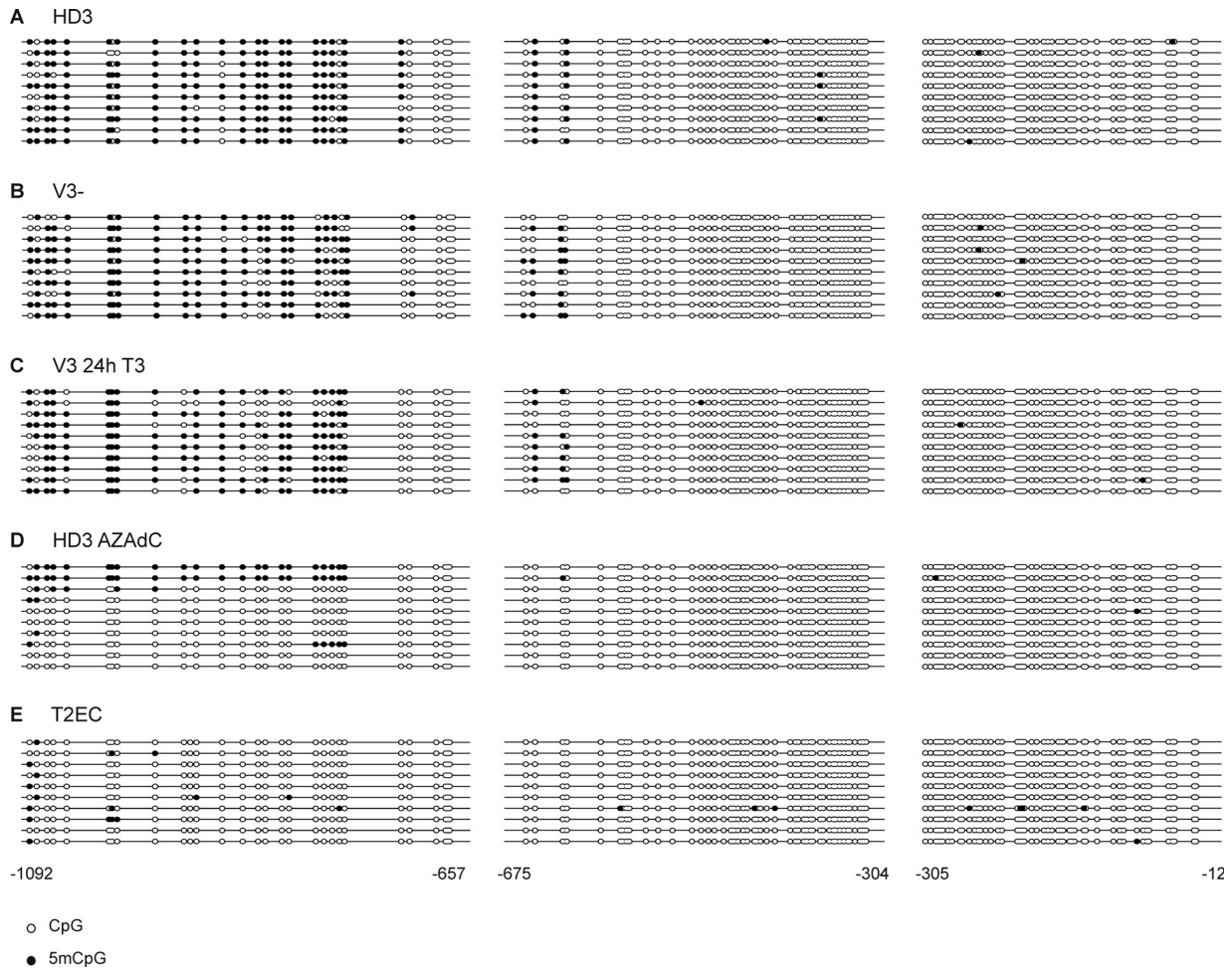

Figure 6. The upstream part of the CAII promoter CpG island is methylated. Bisulphite sequencing analysis of CpG-methylation in (**A**) HD3 cells; (**B**) uninduced V3 cells; (**C**) V3 cells after 24 h of T3 induction; (**D**) HD3 cells after 5 days of AZAdC treatment; and (**E**) T2EC erythrocytic progenitor cells. Genomic DNA was treated as described, PCR-amplified and cloned for sequencing. Individual clones were sequenced. Closed circles, methylated CpG; open circles, unmethylated CpG. Positions relative to the transcription start are indicated.

all modifications were higher than in HD3 cells or ligand-induced V3 cells (compare Figure 8B and C with Figures 2 and 3). In addition, at +6 kb H4 acetylation was considerably higher than in HD3 cells. A transient increase in H4ac at this position was also evident during ligand induction of V3 cells (see Figure 3C). Bisulphite sequencing analysis showed that DNA methylation is largely absent in T2EC cells; only 5% CpG methylation was measured in the upstream part of the CpG island (Figure 6E). We also measured the association of TBP with the CAII promoter. As expected for a (partially) active promoter, TBP was enriched at the transcription start (Figure 8D). Thus, earlier in differentiation under conditions when the CAII promoter is not repressed through AEV transformation, TBP is associated with the CAII promoter, active histone modifications are established and CpG methylation is absent.

DISCUSSION

In this study we characterized the epigenetic code of the CAII locus and in particular its promoter (present within a CpG island) under repressive conditions as well as upon hormone-induced activation. Active histone modifications including H3K9/H4 acetylation and H3K4 tri-methylation are present already under repressive conditions and are localized almost exclusively around the transcription start site. Sequential ChIP experiments showed that these histone marks are primarily present on the same nucleosomes, whereas H3K4me3-containing nucleosomes seem to be devoid of the ubiquitously present H3K9me3. Nevertheless, the individual active marks follow their own individual pattern upon activation of transcription. Within the upstream part of the CpG island active histone modifications are absent and the DNA is hypermethylated. However, H3K9me3 is only slightly higher within the hypermethylated region. DNA hypermethylation is almost completely maintained upon activation of transcription by T3 ligand. Even more strikingly, treatment with AZAdC does not cause drastic changes in positioning of the active histone marks, suggesting that DNA hypermethylation and the association of the previously reported MeCP2–Sin3 complex are not the critical factors in establishing or maintaining a chromatin boundary. The lack of DNA methylation-spreading may instead be the consequence of a

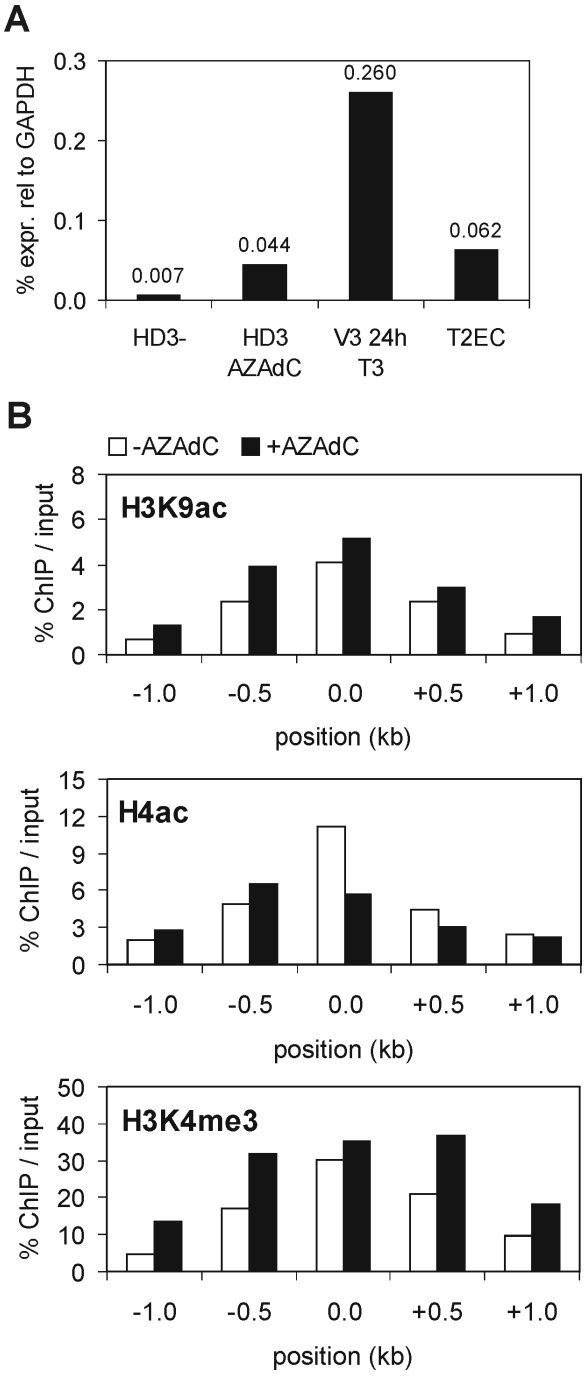

Figure 7. Analysis of active histone modifications after 5 days of AZAdC treatment. (**A**) Comparison of CAII transcription levels under various conditions by real-time RT–PCR using intronic primers. (**B**) Analysis of active histone modification changes after AZAdC treatment. Positions relative to the transcription start site are indicated.

boundary formed by local and high levels of active histone marks. Indeed, chromatin boundaries between escape genes and X-inactivated genes have been shown to contain high levels of localized acetylation (29). Here, the zinc-finger protein CTCF is involved in boundary formation, and it is possible that CTCF also plays a role at the CAII locus.

Although H3K4 tri-methylation is generally regarded as an indicator for active chromatin transcription, the level of H3K4 tri-methylation level does not correlate with CAII promoter activity, and its presence does not necessarily signal ongoing transcription. We have made similar observations for unexpressed genes at the human X-chromosome (11). Moreover, H3K4 tri-methylation is not subjected to significant alteration upon transcriptional activation, but instead is high in both the repressive and active state. Next to marking active chromatin, H3K4 tri-methylation may well mark promoters that become activated and provide the epigenetic setting to facilitate such future activation.

Our results show that PIC assembly is inhibited notwithstanding the active histone modifications at the CAII promoter. This indicates that the establishment of an active epigenetic code alone is insufficient to establish productive transcription. It seems likely that PIC assembly at the promoter is critically regulated through communication with the +7 kb HS2 enhancer which recruits the v-ErbA/NCoR-HDAC complex during repression, and the TRAPP220 co-activator upon activation (19).

Hormone-induced activation of CAII transcription is associated with changes in H3/H4 acetylation, H3K4 tri-methylation, but also nucleosome density, as measured through the association of histone H3. At the transcriptional start site, nucleosome depletion or eviction most likely occurs. This explains why H3/H4ac and H3K4me3 locally decrease during induction, and implicates that the levels of H3K9-Ac and H3K4me3 themselves do not decrease but are—at least partially—maintained. Furthermore, the initial increase in H4 acetylation is in fact even more pronounced. A lowered nucleosome density at the transcriptional start is consistent with our previous observations that ligand induces a DNase I hypersensitive site around the transcriptional start site (26). Since the pan-H3 antiserum does not discriminate between histone H3 and H3.3 histone replacement cannot be excluded. At +7 kb H3 was initially low and slightly decreased even further during T3-induction. This position corresponds with the HS2 DNase I hypersensitive site (19,26). The low levels of H3 measured at the HS2 enhancer strongly suggest that this position is locally devoid of nucleosomes, and explain the low levels of all tested histone modifications at this position (see Figures 2, 3 and 8).

Inhibition of DNA methylation by AZAdC results in modest activation of CAII expression as compared to hormone-induced activation (Figure 7A). Although a significant decrease in CpG methylation is induced at the upstream part of the CpG island (Figure 6D), AZAdC treatment does not cause a positional change of the active histone marks. Instead, a moderate local increase in H3K9 acetylation and H3K4 tri-methylation is evident. The increase in H3K9 acetylation could be the result of the dislodgement of MeCP2-complexed HDACs immediately upstream from the active histone marks. Intrusion of the active epigenetic code into the distal part of the CpG island does not occur, reinforcing the notion of the presence of a boundary or an activity that targets and maintains the active histone marks to a particular position.

In the T2EC erythrocytic progenitor cells the CAII gene is transcribed, the active histone marks are associated with the CAII promoter, but DNA methylation is absent. DNA methylation has apparently occurred later during differentiation, although it is currently unclear whether this also occurs in

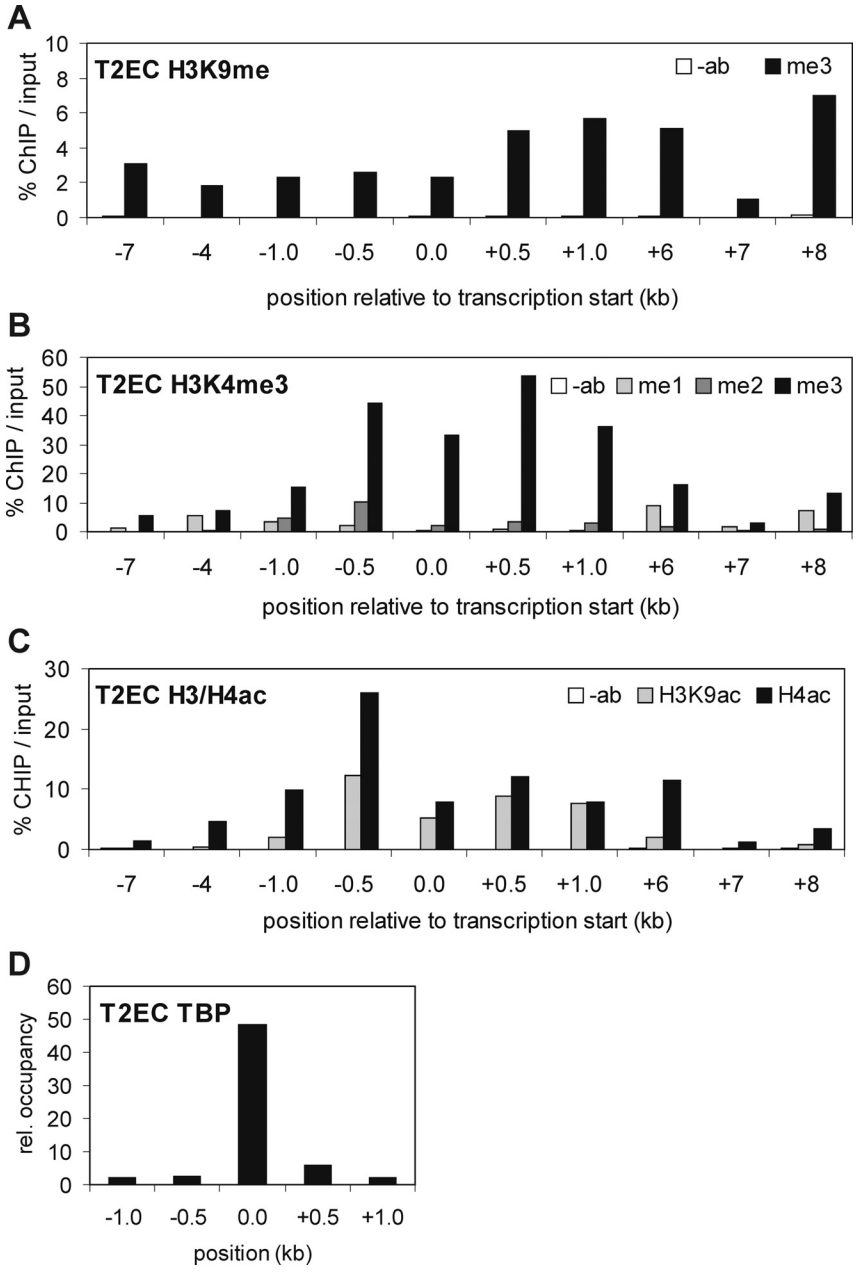

Figure 8. Analysis of active histone modifications in T2EC erythrocytic progenitor cells. (**A**) Histone H3K9me3; (**B**) histone H3K4me1, H3K4me2 and H3K4me3; and (**C**) histone H3/H4 acetylation. (**D**) ChIP analysis of TBP binding in T2EC cells. Values are expressed as occupancy relative to the −7 kb position. Positions relative to the transcription start are indicated.

the animal or whether DNA methylation is due to AEV-induced transformation and/or culturing. DNA methylation has been postulated to be a secondary event that occurs after initial silencing events involving other mechanisms (12). A possible scenario for CAII repression would involve the initial AEV-mediated delivery of a dominant negative v-ErbA that is not responsive to T3. Although this subsequently repressed transcription by inhibiting PIC assembly, it did not lead to histone deacetylation at the promoter. Subsequently, DNA methylation evoked by this repressed state could have progressed towards the CAII promoter, but halted because of the presence of a putative boundary which may involve the active histone marks in addition to other factors. Such factors may include CTCF, which has been shown to protect DNA against *de novo* DNA methylation during imprinting (30), and the combinatorial presence of CTCF and active histone modifications hints to the possibility that they establish a chromatin state that does not permit DNA methylation to spread.

We present here the first example of a bipartite CpG island code, but such codes may be a general phenomenon. Similar local CpG methylation patterns have been described for promoter-containing CpG islands of the mouse and human APRT, ADA and telomerase genes (31), but histone modifications have not been analyzed in these promoters. Whether a bipartite CpG island code is linked to genes that are actively

repressed like CAII remains to be elucidated. Silencing by CpG methylation is believed to involve progressive spreading of DNA methylation, eventually covering entire CpG islands. Our data suggest that boundary elements function as crucial antagonists against such gene silencing events. Whatever the molecular mechanism, the bipartite code within the promoter does not preclude gene activity, and as such it challenges the paradigm that methylation of promoter-containing CpG islands invariantly causes gene silencing.

ACKNOWLEDGEMENTS

We thank Olivier Gandrillon and Sandrine Giraud for providing T2EC cells and related technical advice, Thomas Jenuwein for providing the H3K9(tri-)methyl antiserum, Rolf Ohlsson and members of the Stunnenberg lab for helpful discussions. This research was supported by Dutch Cancer Foundation (KWF) grants KUN 2003-2932 to A.B.B. and KUN 98-1802 to L.E.G.R. Funding to pay the Open Access publication charges for this article was provided by Dutch Cancer Foundation (KWF) grants KUN 2003-2932.

Conflict of interest statement. None declared.

REFERENCES

1. Claus,R. and Lubbert,M. (2003) Epigenetic targets in hematopoietic malignancies. *Oncogene*, **22**, 6489–6496.
2. Brown,R. and Strathdee,G. (2002) Epigenomics and epigenetic therapy of cancer. *Trends Mol. Med.*, **8**, S43–S48.
3. Santos-Rosa,H., Schneider,R., Bannister,A.J., Sherriff,J., Bernstein,B.E., Emre,N.C., Schreiber,S.L., Mellor,J. and Kouzarides,T. (2002) Active genes are tri-methylated at K4 of histone H3. *Nature*, **419**, 407–411.
4. Ng,H.H., Robert,F., Young,R.A. and Struhl,K. (2003) Targeted recruitment of Set1 histone methylase by elongating Pol II provides a localized mark and memory of recent transcriptional activity. *Mol. Cell*, **11**, 709–719.
5. Bernstein,B.E., Humphrey,E.L., Erlich,R.L., Schneider,R., Bouman,P., Liu,J.S., Kouzarides,T. and Schreiber,S.L. (2002) Methylation of histone H3 Lys 4 in coding regions of active genes. *Proc. Natl Acad. Sci. USA*, **99**, 8695–8700.
6. Bernstein,B.E., Kamal,M., Lindblad-Toh,K., Bekiranov,S., Bailey,D.K., Huebert,D.J., McMahon,S., Karlsson,E.K., Kulbokas,E.J., III, Gingeras,T.R. *et al.* (2005) Genomic maps and comparative analysis of histone modifications in human and mouse. *Cell*, **120**, 169–181.
7. Liang,G., Lin,J.C., Wei,V., Yoo,C., Cheng,J.C., Nguyen,C.T., Weisenberger,D.J., Egger,G., Takai,D., Gonzales,F.A. *et al.* (2004) Distinct localization of histone H3 acetylation and H3-K4 methylation to the transcription start sites in the human genome. *Proc. Natl Acad. Sci. USA*, **101**, 7357–7362.
8. Roh,T.Y., Ngau,W.C., Cui,K., Landsman,D. and Zhao,K. (2004) High-resolution genome-wide mapping of histone modifications. *Nat. Biotechnol.*, **22**, 1013–1016.
9. Pokholok,D.K., Harbison,C.T., Levine,S., Cole,M., Hannett,N.M., Lee,T.I., Bell,G.W., Walker,K., Rolfe,P.A., Herbolsheimer,E. *et al.* (2005) Genome-wide map of nucleosome acetylation and methylation in yeast. *Cell*, **122**, 517–527.
10. Schneider,R., Bannister,A.J., Myers,F.A., Thorne,A.W., Crane-Robinson,C. and Kouzarides,T. (2004) Histone H3 lysine 4 methylation patterns in higher eukaryotic genes. *Nature Cell Biol.*, **6**, 73–77.
11. Brinkman,A.B., Roelofsen,T., Pennings,S.W., Martens,J.H., Jenuwein,T. and Stunnenberg,H.G. (2006) Histone modification patterns associated with the human X chromosome. *EMBO Rep.*, **7**, 628–634.
12. Bird,A. (2002) DNA methylation patterns and epigenetic memory. *Genes Dev.*, **16**, 6–21.
13. Jones,P.A. and Baylin,S.B. (2002) The fundamental role of epigenetic events in cancer. *Nature Rev. Genet.*, **3**, 415–428.
14. Baylin,S.B. (2002) Mechanisms underlying epigenetically mediated gene silencing in cancer. *Semin. Cancer Biol.*, **12**, 331–337.
15. Eden,S., Hashimshony,T., Keshet,I., Cedar,H. and Thorne,A.W. (1998) DNA methylation models histone acetylation. *Nature*, **394**, 842.
16. Richards,E.J. and Elgin,S.C. (2002) Epigenetic codes for heterochromatin formation and silencing: rounding up the usual suspects. *Cell*, **108**, 489–500.
17. Feng,Q. and Zhang,Y. (2001) The MeCP1 complex represses transcription through preferential binding, remodeling and deacetylating methylated nucleosomes. *Genes Dev.*, **15**, 827–832.
18. Le Guezennec,X., Vermeulen,M., Brinkman,A.B., Hoeijmakers,W.A., Cohen,A., Lasonder,E. and Stunnenberg,H.G. (2006) MBD2/NuRD and MBD3/NuRD, two distinct complexes with different biochemical and functional properties. *Mol. Cell. Biol.*, **26**, 843–851.
19. Rietveld,L.E., Caldenhoven,E. and Stunnenberg,H.G. (2002) *In vivo* repression of an erythroid-specific gene by distinct corepressor complexes. *EMBO J.*, **21**, 1389–1397.
20. Gandrillon,O., Schmidt,U., Beug,H. and Samarut,J. (1999) TGF-beta cooperates with TGF-alpha to induce the self-renewal of normal erythrocytic progenitors: evidence for an autocrine mechanism. *EMBO J.*, **18**, 2764–2781.
21. Peters,A.H., Kubicek,S., Mechtler,K., O'Sullivan,R.J., Derijck,A.A., Perez-Burgos,L., Kohlmaier,A., Opravil,S., Tachibana,M., Shinkai,Y. *et al.* (2003) Partitioning and plasticity of repressive histone methylation states in mammalian chromatin. *Mol. Cell*, **12**, 1577–1589.
22. Grunau,C., Schattevoy,R., Mache,N. and Rosenthal,A. (2000) MethTools—a toolbox to visualize and analyze DNA methylation data. *Nucleic Acids Res.*, **28**, 1053–1058.
23. Vakoc,C.R., Mandat,S.A., Olenchock,B.A. and Blobel,G.A. (2005) Histone H3 lysine 9 methylation and hp1gamma are associated with transcription elongation through mammalian chromatin. *Mol. Cell*, **19**, 381–391.
24. Litt,M.D., Simpson,M., Gaszner,M., Allis,C.D. and Felsenfeld,G. (2001) Correlation between histone lysine methylation and developmental changes at the chicken beta-globin locus. *Science*, **293**, 2453–2455.
25. Disela,C., Glineur,C., Bugge,T., Sap,J., Stengl,G., Dodgson,J., Stunnenberg,H., Beug,H. and Zenke,M. (1991) v-erbA overexpression is required to extinguish c-erbA function in erythroid cell differentiation and regulation of the erbA target gene CAII. *Genes Dev.*, **5**, 2033–2047.
26. Ciana,P., Braliou,G.G., Demay,F.G., von Lindern,M., Barettino,D., Beug,H. and Stunnenberg,H.G. (1998) Leukemic transformation by the v-ErbA oncoprotein entails constitutive binding to and repression of an erythroid enhancer *in vivo*. *EMBO J.*, **17**, 7382–7394.
27. Gardiner-Garden,M. and Frommer,M. (1987) CpG islands in vertebrate genomes. *J. Mol. Biol.*, **196**, 261–282.
28. Hillier,L.W., Miller,W., Birney,E., Warren,W., Hardison,R.C., Ponting,C.P., Bork,P., Burt,D.W., Groenen,M.A., Delany,M.E. *et al.* (2004) Sequence and comparative analysis of the chicken genome provide unique perspectives on vertebrate evolution. *Nature*, **432**, 695–716.
29. Fillipova,G.N., Cheng,M.K., Moore,J.M., Truong,J.P., Hu,Y.J., Nguyen,D.K., Tsuchiya,K.D. and Disteche,C.M. (2005) Boundaries between chromosomal domains of X inactivation and escape bind CTCF and lack CpG methylation during early development. *Dev. Cell*, **8**, 31–42.
30. Fedoriw,A.M., Stein,P., Svoboda,P., Schultz,R.M. and Bartolomei,M.S. (2004) Transgenic RNAi reveals essential function for CTCF in H19 gene imprinting. *Science*, **303**, 238–240.
31. Cuadrado,M., Sacristan,M. and Antequera,F. (2001) Species-specific organization of CpG island promoters at mammalian homologous genes. *EMBO Rep.*, **2**, 586–592.
32. Li,J. and Leung,F.C. (2006) A CR1 element is embedded in a novel tandem repeat (HinfI repeat) within the chicken genome. *Genome*, **49**, 97–103.